

Electrostatic fluctuations promote the dynamical transition in proteins

Dmitry V. Matyushov*

Center for Biological Physics, Arizona State University, PO Box 871604, Tempe, AZ 85287-1604

Alexander Y. Morozov

Atomic displacements of hydrated proteins are dominated by phonon vibrations at low temperatures and by dissipative large-amplitude motions at high temperatures. A crossover between the two regimes is known as a dynamical transition. Recent experiments indicate a connection between the dynamical transition and the dielectric response of the hydrated protein. We analyze two mechanisms of the coupling between the protein atomic motions and the protein-water interface. The first mechanism considers viscoelastic changes in the global shape of the protein plasticized by its coupling to the hydration shell. The second mechanism involves modulations of the motions of partial charges inside the protein by electrostatic fluctuations. The model is used to analyze mean square displacements of iron of metmyoglobin reported by Mössbauer spectroscopy. We show that high flexibility of heme iron at physiological temperatures is dominated by electrostatic fluctuations. Two onsets, one arising from the viscoelastic response and the second from electrostatic fluctuations, are seen in the temperature dependence of the mean square displacements when the corresponding relaxation times enter the instrumental resolution window.

PACS numbers: 87.14.E-, 87.15.H-, 87.15.kr, 87.10.Pq

Keywords: Dynamical transition, Mössbauer spectroscopy, hydrated protein.

I. INTRODUCTION

Measurements of the Mössbauer absorption of ^{57}Fe in metmyoglobin crystals revealed that the mean square displacement (msd) of this atom starts to grow faster with increasing temperature above $T_D \simeq 200$ K.¹ This finding was followed by similar observations from neutron scattering,² which by now have been reported for a large number of proteins and other biopolymers,³ all demonstrating the same phenomenology.^{4,5} The increase in the slope of the protein msd as a function of temperature was called a “dynamical transition”, presently assigned to a rather broad range of onset temperatures $T_D \simeq 200 - 240$ K. The basic observation is that the high-temperature flexibility of the proteins much exceeds the linear extrapolation of the low-temperature behavior characteristic of an expanding solid. The low-temperature msd is well characterized by the observed phonon spectrum of the protein,⁶ while the high-temperature msd excess is linked to dissipative long-wavelength modes with energies below $\simeq 3$ meV.⁷⁻¹⁰

Early explanations of the dynamical transition offered scenarios ranging from detrapping of the protein conformational motions from low-energy states^{6,11,12} to the glass transition in bulk water.² Several recent observations have shifted the focus to the protein hydration shell. The disappearance of the dynamical transition in dry protein powders,¹³ and its separate existence for the hydration water,^{14,15} point to a strong link between the dynamical transition and the protein hydration shell.

Despite somewhat different semantics, the views in the field seem to converge to the notion of the critical role of the hydration shell in driving the dynamical transition. According to Doster:¹⁶ “The onset of the dynamical transition depends on the solvent viscosity near the pro-

tein surface... The protein-water α -process consists of a concerted librational motion of protein surface residues, coupled to translational jumps of water molecules on the same time scale.” The physical mechanism behind the transition is assigned in this view to the caging of the protein by water’s hydrogen bonds, stiffening its conformational flexibility. As the temperature increases, the population of broken hydrogen bonds grows exponentially, resulting in a release of the protein conformational flexibility in a narrow range of temperatures. Although appealing, this concept does not address the key question of how $\sim 0.5 - 2$ ps events of hydrogen bond breaking develop into a ~ 2 μs collective relaxation process at T_D .

Frauenfelder and co-workers have recently suggested a somewhat different scenario, also focusing on the dynamics of the protein hydration shell.¹⁷⁻¹⁹ According to their view, protein conformations are coupled to motions of the hydration layer, with a relaxation time following an Arrhenius law. This relaxation mode is therefore considered to be a secondary, β -process according to the common classification adopted in the field of supercooled liquids.²⁰ This secondary relaxation is assessed by dielectric spectroscopy of protein samples embedded into solid poly(vinyl)alcohol (PVA), thus eliminating the bulk water relaxation from the dielectric response.^{18,19}

The use of dielectric absorption of PVA-confined proteins yields a surprisingly accurate account of the temperature dependence of the Lamb-Mössbauer factor equal to the fraction of recoilless absorption, $f = \exp[-k_0^2 \langle (\delta x)^2 \rangle]$. Here, $\langle (\delta x)^2 \rangle$ is the msd of the heme iron of metmyoglobin in projection on the wavevector \mathbf{k}_0 of γ -radiation. The iron msd can be separated into a vibrational, low-temperature component $\langle (\delta q)^2 \rangle \propto T$, described by the vibrational density of states (VDOS) of the protein, and a high-temperature component $\langle (\delta Q)^2 \rangle$ appearing at

$T > T_D$. Correspondingly, $f = f_q f_Q$ becomes a product of two components, f_q and f_Q . It turns out that the temperature variation of the Lamb-Mössbauer factor f_Q originating from the high-temperature msd is exceptionally well described by the variance of the sample dipole moment at the same hydration level

$$f_Q = \exp[-k_0^2 \langle (\delta Q)^2 \rangle] = \langle (\delta M)^2 \rangle_< / \langle (\delta M)^2 \rangle. \quad (1)$$

In this equation, $\langle (\delta M)^2 \rangle_<$ is defined as the integral of the frequency-dependent variance of the sample dipole moment M_ω over the frequencies below (subscript “<”) the instrumental frequency $\omega_{\text{obs}} = 1/\tau_{\text{obs}}$, $\tau_{\text{obs}} = 140$ ns.¹⁹ The parameter f_Q then determines the fraction of the sample dipole that has not had a chance to alter on the life-time of the iron nucleus, thus keeping the nuclei in resonance for Mössbauer absorption.

The empirical connection between the dynamical transition and dipolar fluctuations is additionally supported by recent observations of breaks in the dependence of the terahertz dielectric absorption on temperature at typical values of T_D .²¹ All these observations, although advancing the field toward identifying the physical modes responsible for high-temperature flexibility of proteins, pose a significant conceptual challenge.

Both Mössbauer and neutron-scattering techniques probe translational atomic motions on their corresponding resolution windows. It seems therefore natural to relate the break in the temperature dependence of the msd to changes in the dynamic and/or static properties of atomic translations. This is the conceptual framework behind the glass-transition scenario¹⁶ which, even in the current form emphasizing the hydration layer, is focused on the caging arrest, i.e., on the primary effect of short-ranged repulsive interactions in the system. On the contrary, the dielectric measurements^{19,21,22} shift the focus to the long-ranged electrostatic interactions, which is what dielectric spectroscopy is sensitive to at the first place. What is the correct view?

Answering this question requires gaining deeper insights into the actual physical modes coupled to the protein msd at high temperatures, the problem that has evaded direct experimental inquiry so far. Numerical simulations point to enhanced fluctuations of hydrogen bonds of hydration water at high temperatures,²³ but those can be projected on either density or dipolar collective modes. Since a strong link between the dynamical transition and the hydration shell has been clearly established, the main question posed by recent studies is whether density or orientational collective modes drive the transition.²⁴ They are mostly decoupled by symmetry and can therefore be considered as two distinct mechanisms of altering the protein flexibility.

The goal of this paper is to present some initial estimates of the relative importance of the density and orientational fluctuations in the protein dynamical transition. We model the density fluctuations at the protein-water interface by viscoelastic response and the orientational dipolar fluctuations in terms of electrostatic re-

sponse. The dependence of the onset temperature T_D on the observation window is an important ingredient of the observations,^{16,25} which is introduced into the theory by limiting the range of frequencies over which the response functions are integrated,²⁶ similarly to Eq. (1). We start with formulating the model, followed by the results of calculations.

II. MODEL

The purpose of our model is to determine the msd of a single atom, heme iron of metmyoglobin, as a function of temperature. The internal motions of the protein can roughly be separated into two modes, the phonon vibrations \mathbf{q} and dissipative large-scale motions \mathbf{Q} . Even though phonons do not formally exist in proteins, we will use this language to distinguish short-wavelength vibrations from motions altering the protein’s global shape. Accordingly, we will split the coordinate of the iron atom $\mathbf{r} = \mathbf{q} + \mathbf{Q}$ into two statistically independent components, \mathbf{q} and \mathbf{Q} . The former can be expanded in protein’s normal modes or directly calculated from the VDOS measured, for instance, by the phonon-assisted Mössbauer scattering.^{6,27,28} The corresponding msd of the vibrational coordinate \mathbf{q} is, in the classical limit, a linear function of temperature

$$\langle (\delta q)^2 \rangle = a_q T. \quad (2)$$

The proportionality coefficient a_q is calculated from the VDOS according to the standard prescriptions.

The dissipative motions of the protein are seen in neutron scattering spectra as a quasielastic peak with energies below $\simeq 4$ meV, growing in intensity with increasing temperature.⁹ With the sound velocity in a protein^{8,29} of $\simeq 1700$ m/s, the wavelength of the corresponding vibrations is about 26 Å, which is comparable with the diameter of myoglobin, $2R = 36$ Å. These modes therefore alter the global shape of the protein, which is the domain of the viscoelastic response.

In order to obtain a first-order estimate of the geometry changes involved, we will model the protein motions as radial viscoelastic vibrations of a sphere of radius R immersed in a viscoelastic water continuum. The low-frequency variance of the iron coordinate is then simply related to the radius fluctuations of the sphere as $\langle (\delta Q^2) \rangle = (r/R)^2 \langle (\delta R)^2 \rangle$. The latter can be found by solving the standard equations of viscoelasticity^{30,31} yielding the response function $\chi_R(\omega)$ connecting the change of the sphere’s radius R to an oscillatory pressure $p(t) = p_0 e^{i\omega t}$ applied to the sphere’s surface. The result is³⁰

$$\chi_R(\omega) = -\frac{1}{4\pi R} \frac{1}{3\Delta K_p(\omega) + 4\mu_w(\omega)}. \quad (3)$$

Here, $\Delta K_p(\omega) = K_p(\omega) - K_{p,0}$ is the viscoelastic bulk modulus of the protein minus its bulk modulus $K_{p,0}$ at

zero frequency. Further, $\mu_w(\omega)$ is the shear modulus of water. Applying the fluctuation-dissipation theorem³² to Eq. (3), one gets

$$\langle(\delta Q_\omega)^2\rangle = -\frac{2k_B T r^2}{3\omega V_p} \text{Im} \frac{1}{3\Delta K_p(\omega) + 4\mu_w(\omega)}, \quad (4)$$

where V_p is the protein volume.

We now proceed to calculating the Lamb-Mössbauer factor^{33,34}

$$f = \langle | \langle e^{ik_0 x} \rangle |^2 \rangle_{\text{het}}, \quad (5)$$

where $x = \hat{\mathbf{k}}_0 \cdot (\mathbf{q} + \mathbf{Q})$ is the projection of the iron displacement on the direction of photon propagation, $\hat{\mathbf{k}}_0 = \mathbf{k}_0/k_0$. There are two averages in this definition: the inner angular brackets denote an ensemble average over the protein and water modes affecting the position of iron in a single protein, while the outer angular brackets denote the average over the proteins in the sample. This second average carries the subscript ‘‘het’’ to emphasize that it reflects the heterogeneity of the sample, such as for instance variations in the hydration level among different proteins in the protein powder. We do not consider the heterogeneous average in our present study and limit ourselves by the inner average only. This approximation amounts, in experimental techniques, to considering the narrow feature of the Mössbauer absorption line and subtracting the broad base-line originating from the sample heterogeneity.⁶ Accordingly, the experimental points shown in Fig. 1 are obtained from the area $f(T)$ of the narrow line as $-\ln f(T)/(k_0)^2$, $k_0 = 53.2 \text{ \AA}^{-1}$.

The ensemble average over the water/protein statistical distribution can be described in terms of the free energy $F(x)$ such that the inner brackets in Eq. (5) become

$$\langle e^{ik_0 x} \rangle = Z^{-1} \int e^{ik_0 x - \beta F(x)} dx, \quad (6)$$

where $\beta = 1/(k_B T)$ and $Z = \int \exp[-\beta F(x)] dx$. The free energy $F(x)$ is determined by projecting³⁵ the manifold of \mathbf{q} and \mathbf{Q} coordinates on the single coordinate x

$$e^{-\beta F(x)} = \int \delta[x - \hat{\mathbf{k}}_0 \cdot (\mathbf{q} + \mathbf{Q})] \langle e^{-\beta H_0(\mathbf{q}, \mathbf{Q}) - \beta z \phi_w(\mathbf{q}, \mathbf{Q})} \rangle_w d\mathbf{q} d\mathbf{Q}. \quad (7)$$

In this equation, $H_0(\mathbf{q}, \mathbf{Q})$ is the Hamiltonian of classical harmonic vibrations of the protein and ϕ_w is the electrostatic potential of the surrounding dielectric medium acting on the heme iron carrying charge z . The subscript ‘‘w’’ in Eq. (7) specifies water as the main source of the electrostatic fluctuations. It is not, however, required by the theory, and slow protein motions, not included in the calculation of $\langle(\delta q)^2\rangle$, can contribute to the fluctuations of the electrostatic potential as well (see below).

The Hamiltonian $H_0(\mathbf{q}, \mathbf{Q})$ can be given in the Gaussian form

$$\beta H_0(\mathbf{q}, \mathbf{Q}) = \frac{\delta q^2}{2\langle(\delta q)^2\rangle} + \frac{\delta Q^2}{2\langle(\delta Q)^2\rangle}, \quad (8)$$

where the variance of \mathbf{q} is given by Eq. (2) and the variance of \mathbf{Q} requires additional explanation.

The limited instrumental time τ_{obs} affects the observables and, in fact, the dynamical transition itself becomes possible only when the relaxation time of a collective mode of the hydration shell coupled to high-temperature protein’s motions enters the experimental observation window.^{16,19} Therefore, the variance of the slow dispersive motions of the heme iron is not a thermodynamic variable referring to an infinite observation window, but a property affected by instrumental resolution.^{26,36} This is reflected by the subscript ‘‘>’’ in Eq. (8) which indicates that $\langle(\delta Q)^2\rangle_>$ is calculated by integrating the response function in Eq. (4) over the frequencies exceeding the observation frequency $\omega_{\text{obs}} = \tau_{\text{obs}}^{-1}$

$$\langle(\delta Q)^2\rangle_> = \int_{\omega_{\text{obs}}}^{\infty} \langle(\delta Q_\omega)^2\rangle (d\omega/\pi). \quad (9)$$

The statistical average over the electrostatic fluctuations can be simplified by a first-order expansion of the potential ϕ_w in x : $\phi_w(\mathbf{q}, \mathbf{Q}) \simeq \phi_{w,0} - x E_w$, where $\phi_{w,0}$ is the potential at the equilibrium position of iron and E_w is the electric field projected on $\hat{\mathbf{k}}_0$. Assuming that E_w is a Gaussian variable, one gets a Gaussian form of $\beta F(x) = x^2/(2\langle(\delta x)^2\rangle)$ where the variance $\langle(\delta x)^2\rangle$ is

$$\langle(\delta x)^2\rangle = \langle(\delta x)^2\rangle_{\text{el}}/M_E. \quad (10)$$

Here, the elastic msd $\langle(\delta x)^2\rangle_{\text{el}} = \langle(\delta q)^2\rangle + \langle(\delta Q)^2\rangle_>$ is the sum of two statistically decoupled components. Further, the correction M_E represents softening of atomic vibrations by electrostatic fluctuations of the hydration shell.

Similarly to the viscoelastic effect, the electrostatic softening depends on the observation window. Accounting again for the frequency cutoff introduced by the finite instrumental resolution, it is given in the form

$$M_E = 1 - (\beta z)^2 \langle(\delta x)^2\rangle_{\text{el}} \int_{\omega_{\text{obs}}}^{\infty} C_E(\omega) d\omega / (2\pi), \quad (11)$$

where $C_E(\omega)$ is the Fourier transform of the time autocorrelation function of the field $E_w(t)$

$$C_E(\omega) = \int_{-\infty}^{\infty} \langle \delta E_w(t) \delta E_w(0) \rangle e^{i\omega t} dt. \quad (12)$$

By applying the fluctuation-dissipation theorem³² once again, one can recast Eq. (11) in terms of the response function $\chi_E(\omega)$ representing the polar response to an oscillating dipole probe $m(t) = m_0 \exp(i\omega t)$ placed at the position of the iron atom

$$M_E = 1 - \beta z^2 \langle(\delta x)^2\rangle_{\text{el}} \int_{\omega_{\text{obs}}}^{\infty} \chi_E''(\omega) d\omega / (\pi\omega). \quad (13)$$

This form of the correction factor accounting for the dipolar fluctuations of the water shell is used in the calculations below.

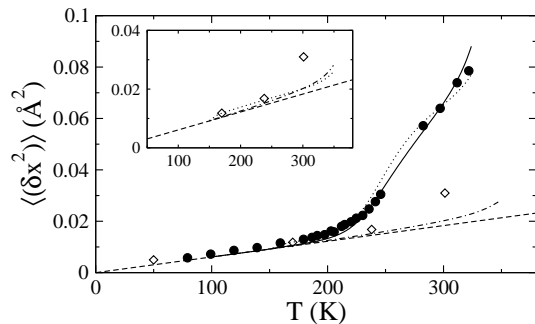


FIG. 1. Temperature dependence of the msd of iron in metmyoglobin. Experimental msd⁶ are shown by circles. Diamonds refer to the msd calculated from the VDOS measured from phonon-assisted Mössbauer effect at different temperatures,⁶ whereas the dashed line is the same calculation from the VDOS at 235 K.²⁷ The dash-dotted line refers to the msd combining phonons with viscoelastic oscillations of the protein shape and the solid line refers to the combination of all three effects: protein's phonons, viscoelastic shape oscillations, and dipolar fluctuations of the hydration layer. The solid line is obtained with $\Delta K_p(T)$ as explained in the text, while the dotted lines refer to the temperature-independent $\Delta K_p = 3.2$ GPa obtained from the fit of Eq. (17) to the protein intrinsic compressibility at 298 K.³⁷ The inset shows the rise of the msd due to the elastic motions near the glass transition temperature of the protein, $T_g \approx 180 \pm 15$ K.

III. MEAN SQUARE DISPLACEMENT

Here we outline the calculations performed using the model developed in this paper. We need to mention that many parameters entering the model are not experimentally available. Some of them can be potentially extracted from numerical simulations. The usefulness of simulations is, however, limited for interpreting the experimental data since reproducing heterogeneous conditions of partially hydrated protein powders presents significant challenges to simulation protocols. Likewise, the viscoelastic model used here should be viewed as only a first step toward a more realistic description of the elastic response of hydrated proteins. However, one of the major conclusions of this paper is the dominance of electrostatics in the high-temperature flexibility of proteins and a relatively small effect of viscoelastic motions on the iron msd. This observation puts high priority to the development of the electrostatic component of the model, and makes the limitations of the modeling of the viscoelastic response less critical.

The viscoelastic response functions entering Eq. (3) were taken in the Maxwell form³²

$$\begin{aligned} \Delta K_p(\omega) &= \frac{\Delta K_p i\omega\tau_p(T)}{1 + i\omega\tau_p(T)}, \\ \mu_w(\omega) &= \frac{G_\infty i\omega\tau_w(T)}{1 + i\omega\tau_w(T)}. \end{aligned} \quad (14)$$

In this equation, $\Delta K_p = K_{p,\infty} - K_{p,0}$ is the change in the bulk protein modulus between infinite and zero fre-

quencies and G_∞ is the high-frequency shear modulus of water; $\tau_{p,w}(T)$ are the corresponding relaxation times. From the Maxwell equation, one gets the shear viscosity $\eta_w(T) = G_\infty(T)\tau_w(T)$ which is well tabulated down to the water nucleation temperature.³⁸ The shear relaxation time was obtained from $\eta_w(T)$ and $G_\infty(T)/\text{GPa} = 1.68 - 0.0127(T - 273)$ taken from Ref. 39. The resulting $\tau_w(T)$ turns out to be close to the exponential relaxation time of the longitudinal modulus extracted from inelastic x-ray scattering:⁴⁰ $\tau_\ell(T)/\text{s} = 0.84 \times 10^{-15} \exp(1910 \text{ K}/T)$.

The VDOS of metmyoglobin powders is well established by phonon-assisted Mössbauer measurements,^{6,8,27} and the temperature slope a_q in Eq. (2) was calculated from the experimental VDOS (dashed line in Fig. 1). Figure 1 also shows a rise in the msd due to the onset of viscoelastic oscillations of the protein (dash-dotted line). These results were obtained by adopting Eq. (14) for the elastic moduli with the protein's relaxation time $\tau_p(T)$ from the measurements done on dry protein powders.²² The relaxation process in dry proteins is too slow to enter the observation window of the spectrometer and $\Delta K_p(\omega) \simeq \Delta K_p$ in Eq. (14).

This notion implies that the frequency dependence of the moduli, e.g., Debye vs dispersive relaxation does not significantly affect the outcome of the calculations and only $\Delta K_p(T)$ matters for the temperature dependence of the viscoelastic msd. The latter was adopted to reproduce the experimental intrinsic compressibility⁴¹ of myoglobin³⁷ $\beta_T = 11.04 \text{ Mbar}^{-1}$ at $T = 298$ K and the temperature variation of Young's moduli of myoglobin crystals at lower temperatures^{42,43} (see below). The use of experimental compressibility to parametrize the model also implies that the overall viscoelastic component of atomic displacements is limited by the thermodynamic experimental value and can only be lower for a given instrumental observation window.

The most uncertain part of our analysis is the calculation of the electric field response function $\chi_E(\omega)$. It can be calculated by solving the Poisson equation for the heme immersed in the heterogeneous dielectric formed by the protein and its hydration layer. However, the assignment of the dielectric constants to both the protein and the thin layer of water surrounding it in the powder is subject to significant uncertainties. We will therefore restrict ourselves to rough estimates aimed to establish whether electrostatic fluctuations can produce a significant effect on the msd under a reasonable set of assumptions. The results of fitting are additionally supported by Molecular Dynamics simulations of the fully hydrated metmyoglobin.⁴⁴

The dielectric response to charges immersed in a polar medium is dominated by longitudinal modes of dipolar polarization⁴⁵ characterized by the dielectric modulus $\epsilon(\omega)^{-1}$, where $\epsilon(\omega)$ is the complex, frequency-dependent dielectric constant of the protein-water mixture. The dielectric response function $\chi_E(\omega)$ establishes the reaction field of the dielectric medium in response to a probe dipole placed at the position of the heme iron. It scales as

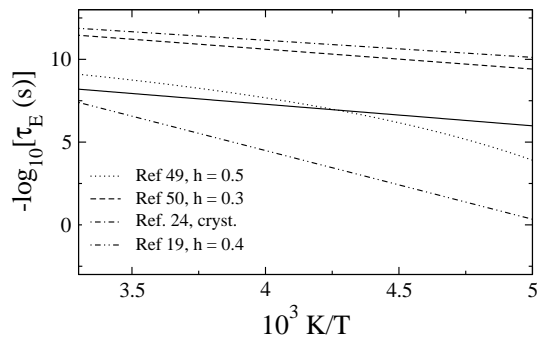


FIG. 2. Dielectric longitudinal relaxation time $\tau_L(T) = (\epsilon_\infty/\epsilon_s)\tau_E(T)$ reported in the literature^{19,47,48} with the protein hydration levels indicated in the legend. The results from Ref.¹⁹ refer to myoglobin confined in PVA, results from Ref.²⁴ are for metmyoglobin crystals, and Refs.^{47,48} refer to metmyoglobin powders. The solid line refers to the longitudinal, Debye relaxation time of the reaction field response function $\chi_E(\omega)$ [Eq. (16)], $\tau_L(T)/s = 3.2 \times 10^{-13} \exp[3000 \text{ K}/T]$, used to fit the experimental msd for the heme iron.⁶

the inverse cube of the characteristic size d of the heme. The loss function $\chi_E''(\omega)$ can therefore be written in the form

$$\chi_E''(\omega) = \frac{1}{d^3} \frac{\epsilon''(\omega)}{|\epsilon(\omega)|^2}. \quad (15)$$

Dielectric properties of partially hydrated proteins have not been well characterized since the results are strongly affected by both the sample preparation and the hydration level. Even dielectric relaxation times measured on samples of close hydration level are rather inconsistent. This point is illustrated in Fig. 2 where results on partially hydrated myoglobin powders of hydration level $h = 0.3 - 0.5$ (in g of water per g of protein) have been assembled.^{19,46-48} We also show measurements done on myoglobin crystals²⁴ for the sake of comparison. Multiple relaxation processes are common for such measurements, and the fastest relaxation, commonly attributed to the hydration shell,^{22,47} is shown in Fig. 2.

Even if we could firmly establish the proper relaxation time for the the sample dipole moment, this would not necessarily give us the relaxation time of the reaction field correlation function required for $\chi_E''(\omega)$. Because of the linear scaling of the dipole moment variance with the number of dipoles, dielectric measurements emphasize the effect of outer solvation shells, while $\chi_E''(\omega)$ is dominated by waters closest to the probe dipole (heme's iron). In view of these uncertainties, we have constructed the temperature-dependent relaxation time $\tau_E(T)$ that, together with the parameter d in Eq. (15), allows us to fit the experimental msd.

Assuming the Debye form for the fast relaxation component in $\epsilon(\omega)$,^{22,48} the response function in Eqs. (13) and (15) gains the form

$$\beta z^2 \chi_E''(\omega) = \frac{1}{\delta^2} \frac{\omega \tau_L}{1 + (\omega \tau_L)^2}, \quad (16)$$

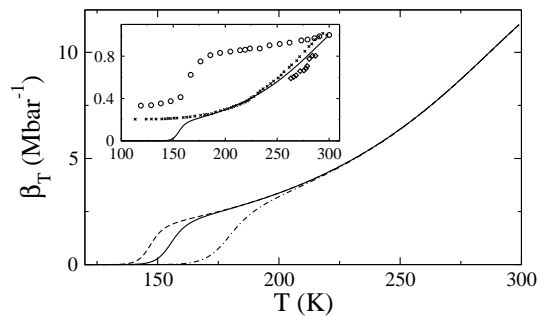


FIG. 3. Intrinsic isothermal compressibility $\beta_T(T)$ of a protein calculated from Eq. (17) with $\omega_{\text{obs}} = 1$ (dashed line), 10^2 (solid line), and 10^3 MHz (dash-dotted line). The protein and water parameters are those adopted for the calculation of the myoglobin msd, with $\Delta K_p(T)/\text{GPa} = 3.22 - 0.03 \times (T - 298) + 0.00025 \times (T - 298)^2$ obtained to fit the protein intrinsic compressibility at 298 K³⁷ and the temperature dependence of Young's moduli (crosses in the inset). The inset shows experimental expansivity of the hydration shell of lysozyme (circles),⁵¹ experimental inverse Young's moduli of myoglobin crystals exposed to air of 95–100% (diamonds)⁴³ and 75% humidity (crosses).⁴² The solid line shows $\beta_T(T)$ calculated from Eq. (17) at $\omega_{\text{obs}} = 10^2$ MHz; all curves are normalized to the corresponding values at $T = 298$ K.

where the parameter δ , $\delta^{-2} = \beta z^2 c_0 / d^3$ sets up a characteristic length and $c_0 = \epsilon_\infty^{-1} - \epsilon_s^{-1}$ is the Pekar factor. In addition, $\tau_L = (\epsilon_\infty/\epsilon_s)\tau_E$ is the longitudinal dielectric time and ϵ_∞ and ϵ_s are the high-frequency and static dielectric constants, respectively. The parameters $\delta = 0.12$ Å and $\tau_L(T)/s = 3.2 \times 10^{-13} \exp[3000 \text{ K}/T]$ (solid line in Fig. 2) were used in fitting the experimental msd. The fitting relaxation time $\tau_L(T)$ is generally consistent with dielectric measurements and, in addition, the Arrhenius slope of $\tau_L(T)$ matches our simulations of the protein Stokes-shift dynamics at elevated temperatures.⁴⁹ More detailed calculations might require replacing one-relaxation Debye dynamics in Eq. (16) with dispersive dynamics characterized by a distribution of relaxation time, as suggested by the NMR experiment.⁵⁰

The overall fluctuations of the protein volume are determined by the response function in Eq. (3) combining the dynamic elastic moduli of the protein and the hydration shell. This connection can be used to parameterize the model on volumetric properties of hydrated proteins, in particular on protein's intrinsic compressibility.⁴¹ For a given instrumental resolution, one obtains from Eq. (3) for the isothermal compressibility $\beta_T \propto \langle (\delta V_p)^2 \rangle$ of the protein

$$\beta_T = -(6/\pi) \int_{\omega_{\text{obs}}}^{\infty} \text{Im} [3\Delta K_p(\omega) + 4\mu_w(\omega)]^{-1} (d\omega/\omega). \quad (17)$$

In Fig. 3 we show $\beta_T(T)$ for the parameters adopted in the calculations of the iron msd and several values of ω_{obs} . The intrinsic compressibility of the protein rises sharply at the point close to protein's glass transition T_g . The latter depends on the observation window, but

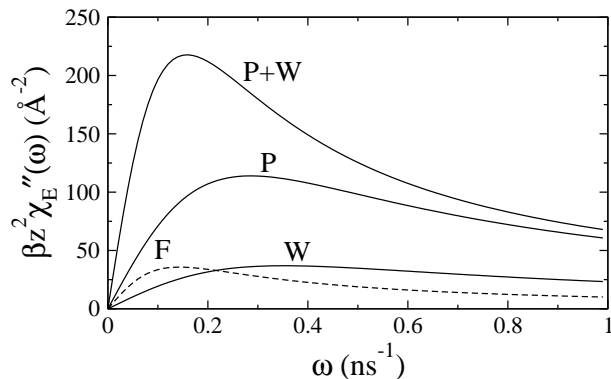


FIG. 4. The loss function $\beta z^2 \chi_E''(\omega)$ obtained from the fitting of the experimental msd to Eqs. (10), (13), and (16) (marked as “F”) and from direct MD simulations of the electric field acting on the iron of metmyoglobin. The plot shows the result for the overall electric field produced by protein and water (“P+W”) and by protein (“P”) and water (“W”) separately. The simulation trajectories ($T = 300$ K) were 45 ns long, 35 ns of which were used for collecting the correlation functions.⁴⁴

is close to reported values $T_g \simeq 180 \pm 15$ K^{43,51,52} marked by breaks in several observable parameters.⁵² The rise of compressibility at T_g in our calculations is caused by the water component of the viscoelastic response function when the relaxation time τ_w becomes smaller than τ_{obs} . This result is consistent with the glass transition of the hydration shell expansivity⁵¹ shown in the inset in Fig. 3. The inset in Fig. 3 also shows compressibilities obtained from experimentally reported Young’s moduli of myoglobin crystals^{42,43} assuming that their Poisson ratios are independent of temperature. The temperature variation of $\Delta K_p(T)$ in our calculations shown in Fig. 1 was chosen to match these data.

The fit of $\Delta K_p(T)$ to crystalline Young’s moduli results in an upward increase of the elastic msd at the highest temperatures shown in Fig. 1. This upward increase reflects pre-melting of myoglobin crystals when their Young’s moduli approach zero.⁴³ Since the melting temperature is typically higher in protein powders,⁴³ $\Delta K_p(T)$ obtained from fitting the crystal data might overestimate these effects; the iron msd with a temperature-independence $\Delta K_p = 3.2$ GPa is shown by the dotted line in Fig. 1.

The results shown in Fig. 1 indicate that electrostatic fluctuations far outweigh viscoelastic vibrations in the iron msd. We additionally confirm this outcome by comparing the function $\beta z^2 \chi_E''(\omega)$ from our fitting to the same function obtained from MD simulation of the fully hydrated metmyoglobin.⁴⁴ Figure 4 shows the response functions from the electric field fluctuations produced by the protein and water combined and by each component separately. The height of the maximum quantifies the strength of the msd modulation by the corresponding electrostatic component, and it is of main importance for this comparison.

We have assumed so far that the protein is electrostatically

non-polar, and its hydration shell is the main source of the electrostatic fluctuations. It does not need to be so. Low-frequency motions, not included in the VDOS used to calculate $\langle(\delta q)^2\rangle$, can modulate the protein’s partial charges (dipole moments of α -helices, ionized surface residues, etc.) and compete in the electrostatic noise with the hydration layer. This might be particularly true for partially hydrated protein powders where the fluctuations of the water dipoles are probably reduced to motions of polarized domains around ionized surface residues.

Figure 4 in fact shows that the protein component of $\chi_E''(\omega)$ exceeds that of water, and its maximum is higher than that of the fitting function from Eq. (16). The electrostatic fluctuations of the protein itself are therefore sufficient to produce the observable msd and, in addition, our estimates do not seem to overestimate the effect of the electrostatic fluctuations on the msd. The primary role of water in powders might be reduced to ionizing the surface residues of the protein and plasticizing its motions above T_g (Fig. 3). Water in patches solvating ionized residues is strongly coupled to the protein both electrostatically and by surface hydrogen bonds. The relaxation times of their electrostatic response functions are therefore close (Fig. 4), resulting in matching onset temperatures of the dynamical transition for each component.^{14,15}

Further, the overall loss function $\chi_E''(\omega)$, which includes cross-correlations between the water and protein electric fields, shows a slower relaxation time than each component separately. The relaxation time of 6.3 ns of the essentially Debye overall function $\chi_E''(\omega)$ is close to $\tau_L(300 \text{ K}) \simeq 7$ ns adopted in fitting of the experimental msd. It is this loss function, combining the protein and water electrostatics, that is of primary interest for the modeling of the high-temperature flexibility of proteins.

IV. DISCUSSION

The picture presented here assigns an increase in the protein msd at the dynamical transition to the entrance of a collective relaxation time of the protein-water interface into the observation window of the spectrometer.^{19,22,53} We consider two types of interfacial fluctuations, elastic modes changing the global shape of the protein and electrostatic fluctuations. Electrostatics turn out to be the main factor affecting the high-temperature portion of the msd.

The longitudinal relaxation time of the electric field fluctuations, $\tau_L(T)$, determines the transition temperature by the condition $\omega_{\text{obs}} \tau_L(T_D) \simeq 1$. With the Arrhenius form for the relaxation time $\tau_L(T)$, this condition predicts a logarithmic dependence of T_D on the observation frequency,

$$T_D \propto |\ln[\omega_{\text{obs}} \tau_0]|^{-1}, \quad (18)$$

where τ_0 is the preexponent in $\tau_L(T)$. For instance, with

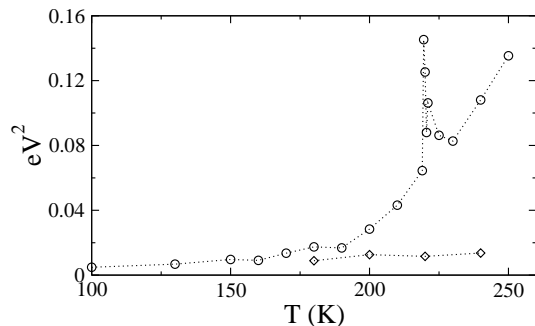


FIG. 5. Variance of the water’s electrostatic potential at the active site, $\Delta q^2 \langle (\delta\phi)^2 \rangle$ of the protein plastocyanin from MD simulations (circles).⁵⁵ Diamonds show the difference of water potentials in equilibrium with the active site carrying charges q_1 and q_2 , $\beta^{-1} \Delta q (\langle \phi \rangle_1 - \langle \phi \rangle_2)$, $\Delta q = q_2 - q_1$. This latter quantity is sensitive to high-frequency ballistic modes of the hydration water, but not to collective fluctuations of the shell dipole.⁵⁶ The two calculations coincide in the linear response approximation, which is valid at low temperatures. Linear response breaks down when the collective mode of water’s dipolar polarization enters the observation window fixed by the length of the simulation trajectory. The spike at $\simeq 220$ K in the potential variance carries signatures of a weak first-order transition, but its origin is currently unclear.

the observation window of neutron scattering of $\simeq 500$ ps and of Mössbauer spectroscopy of 140 ns, the above equation yields 1.4 for the ratio of T_D values measured by neutron and Mössbauer techniques ($\tau_0 = 10^{-13}$ s). This estimate assumes equal electrostatic relaxation times for (mostly surface) protons and heme iron, which is likely not true. The actual picture is also more complex as several slope changes contribute to the overall temperature dependence of the msd.⁵⁴ It is also the case with the present model producing two different onsets arising from viscoelastic and electrostatic fluctuations. An increase in T_D was also reported for proteins solvated in glycerol and in concentrated sucrose-water solutions.¹⁶ Although an increase in viscosity does shift T_D in the right direction according to Eq. (18), the alteration of the effective polarity of the hydration layer and the surface charge distribution of the protein might be other factors contributing to the shift. Generally, the the present model predicts a decrease in the protein atomic displacements for hydration in solvents of lower polarity.

The main physical question looming behind the phenomenon of the dynamical transition is what are the mechanisms and physical modes allowing high flexibility of proteins at physiological temperatures. We emphasize here electrostatic fluctuations as the primary origin of the increase in the protein’s atomic displacements. This mechanism connects the translational manifold of the protein’s interior to the dipolar orientational manifold of the hydration layer. While this connection was established empirically by experiment [Eq. (1)], numerical

simulations directly show the same basic phenomenology for the electrostatic fluctuations and the atomic msd.

Figure 5 shows the results of numerical simulations for the variance of the electrostatic potential produced by the water hydration shell at the active site of the protein plastocyanin.⁵⁵ A break in the temperature dependence at T_D refers to the time-scale of $\simeq 10$ ns fixed by the length of the simulation trajectory. The difference of the first moments of the potential in the two redox states of the protein (diamonds in Fig. 5) gives the component of the same property produced by the ballistic dynamics of the hydration shell and not sensitive to its collective relaxation.⁵⁶ In a sense, the diamonds in Fig. 5 are analogs to the diamonds in Fig. 1 referring to the vibrational component of the msd.⁶ There is a clear qualitative similarity between laboratory and numerical results presented in Figs. 1 and 5.

Because the response function of the water’s electric field scales as d^{-3} with the distance d from the surface inside the protein, dipolar fluctuations of the hydration shell will mostly affect protein’s surface residues. The vibrations of the surface protons will therefore be softer than of interior protons, and they will stronger contribute to the observable msd. There is also a possibility of “surface melting” when $M_E = 0$ in Eq. (10) is reached with rising temperature for a group of atoms. The low-temperature conformation of the corresponding residues will become unstable, with the instability released through a conformational transition.

The present model predicts higher flexibility for atoms carrying higher partial charges. In case of heme iron this implies higher flexibility of the protein oxidized state compared to the reduced state. While this prediction qualitatively agrees with experiment,^{57,58} more detailed studies are required to distinguish the effect of electrostatic fluctuations from the alteration of the VDOS also occurring upon changing the redox state.

V. CONCLUSIONS

The model proposed here treats high-temperature atomic displacements of the protein as a combination of viscoelastic deformation of the global protein shape and electrostatic fluctuations coupled to the atomic charge. We suggest that electrostatic fluctuations dominate the high-temperature flexibility of proteins.

ACKNOWLEDGMENTS

This research was supported by the National Science Foundation (CHE-0910905). We are grateful to Alexei Sokolov, Jan Swenson, and Guo Chen for communicating results of their dielectric measurements to us. DVM has greatly benefited from useful discussions with Robert Young and Alexei Sokolov.

- * dmitrym@asu.edu
- ¹ F. Parak and H. Formanek, *Acta Crystallogr. A* **27**, 573 (1971).
 - ² W. Doster, S. Cusack, and W. Petry, *Nature* **337**, 754 (1989).
 - ³ G. Caliskan, R. M. Briber, D. Thirumalai, V. Garcia-Sakai, S. A. Woodson, and A. P. Sokolov, *J. Am. Chem. Soc.* **128**, 32 (2006).
 - ⁴ F. Gabel, D. Bicout, U. Lehnert, M. Tehei, M. Weik, and G. Zaccai, *Quat. Rev. Biophys.* **35**, 327 (2002).
 - ⁵ F. G. Parak, *Rep. Prog. Phys.* **66**, 103 (2003).
 - ⁶ F. G. Parak and K. Achterhold, *J. Phys. Chem. Solids* **66**, 2257 (2005).
 - ⁷ M. Diehl, W. Doster, W. Petry, and H. Schober, *Biophys. J.* **73**, 2726 (1997).
 - ⁸ K. Achterhold and F. G. Parak, *J. Phys.: Condens. Matter* **15**, S1683 (2003).
 - ⁹ M. Marconi, E. Cornicchi, G. Onori, and A. Paciaroni, *Chem. Phys.* **345**, 224 (2008).
 - ¹⁰ K. Hinsen and G. R. Kneller, *Proteins* **70**, 1235 (2008).
 - ¹¹ H. Frauenfelder, S. G. Sligar, and P. G. Wolynes, *Science* **254**, 1598 (1991).
 - ¹² G. Zaccai, *Science* **288**, 1604 (2000).
 - ¹³ V. Kurkal, R. M. Daniel, J. L. Finney, M. Tehei, R. V. Dunn, and J. C. Smith, *Chem. Phys.* **317**, 267 (2005).
 - ¹⁴ K. Wood, A. Frölich, A. Paciaroni, M. Moulin, M. Härtle, G. Zaccai, D. J. Tobias, and M. Weik, *J. Am. Chem. Soc.* **130**, 4586 (2008).
 - ¹⁵ X.-Q. Chu, A. Faraone, C. Kim, E. Fratini, P. Baglioni, J. B. Leao, and S.-H. Chen, *J. Phys. Chem. B* **113**, 5001 (2009).
 - ¹⁶ W. Doster, *Biochim. Biophys. Acta* **1804**, 3 (2010).
 - ¹⁷ P. W. Fenimore, H. Frauenfelder, B. H. McMahon, and R. D. Young, *Proc. Natl. Acad. Sci.* **101**, 14408 (2004).
 - ¹⁸ G. Chen, P. W. Fenimore, H. Frauenfelder, F. Mezei, J. Swenson, and R. D. Young, *Phil. Mag.* **88**, 33 (2008).
 - ¹⁹ H. Frauenfelder, G. Chen, J. Berendzen, P. W. Fenimore, H. Jansson, B. H. McMahon, I. R. Stroe, J. Swenson, and R. D. Young, *Proc. Natl. Acad. Sci.* **106**, 5129 (2009).
 - ²⁰ M. D. Ediger, C. A. Angell, and S. R. Nagel, *J. Phys. Chem.* **100**, 13200 (1996).
 - ²¹ Y. He, P. I. Ku, J. R. Knab, J. Y. Chen, and A. G. Markelz, *Phys. Rev. Lett.* **101**, 178103 (2008).
 - ²² S. Khodadadi, S. Pawlus, J. H. Roh, V. G. Sakai, E. Mamonov, and A. P. Sokolov, *J. Chem. Phys.* **128**, 195106 (2008).
 - ²³ M. Tarek and D. J. Tobias, *Phys. Rev. Lett.* **88**, 138101 (2002).
 - ²⁴ G. P. Singh, F. Parak, S. Hunklinger, and K. Dransfeld, *Phys. Rev. Lett.* **47**, 685 (1981).
 - ²⁵ S. Magazù, F. Migliardo, and A. Benedetto, *J. Phys. Chem. B* **114**, 9268 (2010).
 - ²⁶ D. V. Matyushov, *J. Chem. Phys.* **130**, 164522 (2009).
 - ²⁷ K. Achterhold, C. Keppler, A. Ostermann, U. van Bürck, W. Sturhahn, E. E. Alp, and F. G. Parak, *Phys. Rev. E* **65**, 051916 (2002).
 - ²⁸ B. M. Leu, Y. Zhang, L. Bu, J. E. Straub, J. Zhao, W. Sturhahn, E. E. Alp, and J. T. Sage, *Biophys. J.* **95**, 5874 (2008).
 - ²⁹ B. M. Leu, A. Alatas, H. Sinn, E. E. Alp, A. H. Said, H. Yavas, J. Zhao, J. T. Sage, and W. Sturhahn, *J. Chem. Phys.* **132**, 085103 (2010).
 - ³⁰ L. D. Landau and E. M. Lifshits, *Theory of elasticity* (Elsevier, Amsterdam, 1986) p. 18.
 - ³¹ R. M. Christensen, *Theory of Viscoelasticity* (Dover Publications, Inc., Mineola, N. Y., 2003).
 - ³² J. P. Boon and S. Yip, *Molecular Hydrodynamics* (Dover Publications, Inc., New York, 1991).
 - ³³ K. S. Singwi and A. Sjolander, *Phys. Rev.* **120**, 1093 (1960).
 - ³⁴ T. E. Cranshaw, B. W. Dale, G. O. Longworth, and C. E. Johnson, *Mössbauer spectroscopy and its applications* (Cambridge University Press, Cambridge, 1985).
 - ³⁵ P. M. Chaikin and T. C. Lubensky, *Principles of condensed matter physics* (Cambridge University Press, Cambridge, 1995).
 - ³⁶ E. W. Knapp, S. F. Fischer, and F. Parak, *J. Chem. Phys.* **78**, 4701 (1983).
 - ³⁷ K. Mori, Y. Seki, Y. Yamada, and H. M. K. Soda, *J. Chem. Phys.* **125**, 054903 (2006).
 - ³⁸ K. R. Harris and L. A. Woolf, *J. Chem. Eng. Data* **49**, 1064 (2004).
 - ³⁹ W. M. Slie, J. A. R. Donfor, and T. A. Litovitz, *J. Chem. Phys.* **44**, 3712 (1966).
 - ⁴⁰ G. Monaco, A. Cunsolo, G. Ruocco, and F. Sette, *Phys. Rev. E* **60**, 5505 (1999).
 - ⁴¹ D. P. Kharakoz, *Biophys. J.* **79**, 511 (2000).
 - ⁴² V. N. Morozov and S. G. Gevorgian, *Biopolymers* **24**, 1785 (1985).
 - ⁴³ V. N. Morozov and Y. Y. Morozova, *J. Biomol. Struct. Dyn.* **11**, 459 (1993).
 - ⁴⁴ D. V. Matyushov, unpublished.
 - ⁴⁵ D. V. Matyushov, *J. Chem. Phys.* **120**, 1375 (2004).
 - ⁴⁶ J. Swenson, H. Jansson, and R. Bergman, *Phys. Rev. Lett.* **96**, 247802 (2006).
 - ⁴⁷ G. Schirò, A. Cupane, E. Vitrano, and F. Bruni, *J. Phys. Chem. B* **113**, 9606 (2009).
 - ⁴⁸ M. Bonura, G. Schirò, and A. Cupane, *Spectroscopy* **24**, 143 (2010).
 - ⁴⁹ D. N. LeBard, V. Kapko, and D. V. Matyushov, *J. Phys. Chem. B* **112**, 10322 (2008).
 - ⁵⁰ S. A. Lusceac, M. R. Vogel, and C. R. Herbers, *Biochim. Biophys. Acta* **1804**, 41 (2010).
 - ⁵¹ W. Doster, S. Busch, A. M. Gaspar, M.-S. Appavou, J. Wuttke, and H. Scheer, *Phys. Rev. Lett.* **104**, 098101 (2010).
 - ⁵² S. Khodadadi, A. Malkovskiy, A. Kisliuk, and A. P. Sokolov, *Biochim. Biophys. Acta* **1804**, 15 (2010).
 - ⁵³ R. M. Daniel, J. L. Finney, and J. C. Smith, *Faraday Discuss.* **122**, 163 (2002).
 - ⁵⁴ M. Krishnan, V. Kurkal-Siebert, and J. Smith, *J. Phys. Chem. B* **112**, 5522 (2008).
 - ⁵⁵ D. N. LeBard and D. V. Matyushov, *Phys. Rev. E* **78**, 061901 (2008).
 - ⁵⁶ D. N. LeBard and D. V. Matyushov, *J. Phys. Chem. B* **114**, 9246 (2010).
 - ⁵⁷ E. N. Frolov, R. Gvosdev, V. I. Goldanskii, and F. G. Parak, *J. Biol. Inorg. Chem.* **2**, 710 (1997).
 - ⁵⁸ A. M. Jorgenson, F. Parak, and H. E. M. Christensen, *Phys. Chem. Chem. Phys.* **7**, 3472 (2005).